Spin Locked Steady-State Free Precession Imaging

W. R. Witschey[1], A. Borthakur[2], M. Elliott[2], A. Voorhees[3], and R. Reddy[2]

[1]Biochemistry and Molecular Biophysics, University of Pennsylvania, Philadelphia, PA, United States, [2]Radiology, University of Pennsylvania, Philadelphia, PA, United States, [3]Siemens Medical Solutions USA, Inc., Malvern, PA, United States

Introduction: T1ρ MRI is typically performed by magnetization preparation followed by a readout sequence during which the T1ρ-weighted signal is frequency and phase encoded (1). This paradigm is inherently time inefficient and, instead, it might be desirable to continuously acquire the T1ρ-weighted signal in the steady-state. Unfortunately, it isn't clear how to establish a steady-state T1ρ contrast with significant signal, since, on-resonance, the rotating frame thermal polarization is nearly zero with RF fields appropriate for clinical use. On the other hand, the steady-state of an off-resonance spin lock is significant and image acquisition is possible by interleaving an off-resonance spin locking RF pulse train with a short period for data acquisition. In this study, we aimed to develop a steady-state spin locking pulse sequence (slSSFP), which was previously validated in phantoms (2), for use *in vivo*. An unexpected consequence of this work was the similarity of the contrast to bSSFP, such that we additionally compared the slSSFP signal to the well known bSSFP signal as a function of the relaxation times T1 and T2. In addition, grey matter, white matter, CSF contrast was measured in the human brain among 4 volunteers at ultra high field (7T).

Materials and Methods: ***Pulse Sequence Design.*** The pulse sequence used for slSSFP imaging is shown in Figure 1A. An initial preparatory α-pulse was delivered on-resonance to flip the magnetization parallel to the effective field in a rotating frame of reference. The effective field amplitude ($\nu_{eff} = \sqrt{(\nu_1 + \Delta\nu)}$) and direction (tan theta = $\nu_1/\Delta\nu$) was chosen such that its orientation was collinear with the bSSFP steady-state magnetization. The magnetization was locked along the direction of the effective field, interrupted only briefly for a period of data acquisition (Figure 1B). The magnetization trajectory is depicted in two reference frames (Figure C); in a reference frame rotating with the frequency of RF irradiation, the magnetization was fixed along the direction of the effective field, but in a reference frame rotating at the Larmor frequency, the magnetization nutated around the z-axis, accumulating a phase phi = $\Delta\nu$TSL each TR. ***Simulations***. The transient and steady-state magnetization response during slSSFP and bSSFP was simulated using the Bloch equations using an ODE solver. The simulation parameters were TE/TR/τ_{pulse} = 2.5/5/1 ms and T1/T2 = 800/50 ms. bSSFP was constructed by half-alpha preparation and 180° phase alternation of the RF pulse every TR (3). ***MRI.*** 4 volunteers were scanned on a 7T Siemens MRI system equipped with 40 mT/m gradients and an 8-channel head coil with bSSFP and slSSFP using identical imaging parameters: 0.469 mm^2 resolution, FOV = 240 x 165 mm^2, TE/TR = 3.3/7.2 ms, bandwidth = 510 Hz/pixel, matrix = 512 x 392 x 256, slice thickness = 0.7 mm.

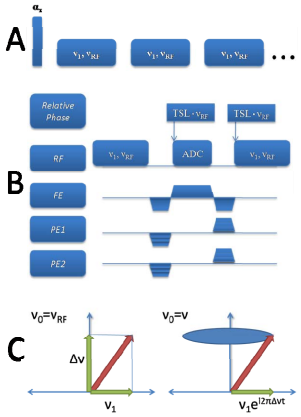

Figure 1: The pulse sequence used for spin locked steady-state free precession imaging.

Results: The magnetization trajectory during the first 200 RF pulses is shown in Figure 2. As expected, for bSSFP, the transverse (Figure 2A) components of the magnetization approach a steady-state condition, which is dependent on T1, T2, TR and α. The trajectory of the magnetization vector can be shown to oscillate between ±α due to phase alternation (Fig. 2C) as has been described before. During slSSFP, the transverse magnetization decays monotonically to the steady state (Figure 2B) allowing for small perturbations during the transient decay to the steady-state. In contrast to the bSSFP magnetization trajectory in Figures 2A and 2C, the trajectory is smooth, since the magnetization is never flipped. The trajectory of the magnetization is very different from bSSFP (Figure 2D). Although the magnetization is initially aligned at an angle α in the y-z plane, the magnetization traces a cone of angle α during RF irradiation. The magnetization decays along this cone in a fashion which is similarly dependent on the relaxation times, repetition time, although the decay appears to be relatively insensitive to RF pulse power if sufficient RF is delivered to overcome relaxation and variations in the static field (the details of this RF power independence are discussed in greater detail in abstract #1270). The dependence on relaxation times T1/T2 was found to be nearly identical (Figure 3). T2-weighted contrast was maximized empirically (2α = 15°) and grey matter, white matter and CSF contrast-to-noise ratio (CNR) were measured in four volunteers at 7T and was 9.4 (GM/WM), 24.6 (GM/CSF) and 34.0 (WM/CSF).

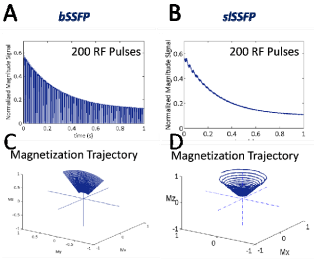

Figure 2: A comparison of the well-known bSSFP trajectory to the slSSFP trajectory .

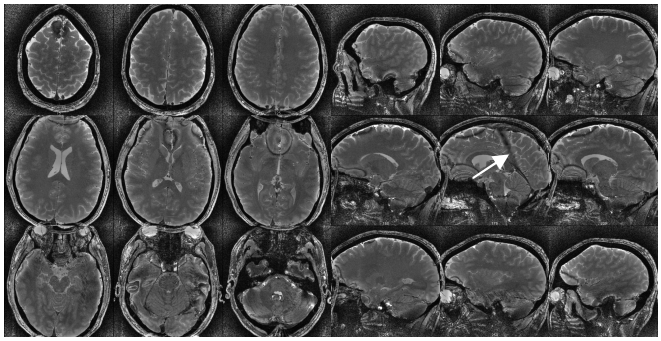

Figure 4: slSSFP brain scanning at 7T. Full brain coverage (0.47 mm^2 x 0.7 mm) with T2-weighting was achieved in approximately 11 minutes. Arrow depicts steady-state artifacts owing to static field variation.

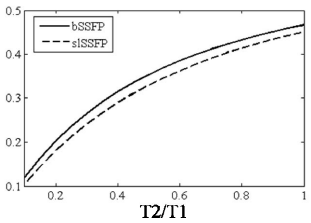

Figure 3: slSSFP dependence on relaxation times. slSSFP exhibits similar T1/T2 contrast to bSSFP.

Discussion: Although simulations were performed in the motional narrowing regime, it is unclear to what extent low frequency relaxation dispersion modifies brain grey matter and white matter contrast. The effects of off-resonance spin lock RF irradiation on image contrast have been previously examined by several authors (4-5). All authors seem to agree that with fixed RF amplitude, there is a tradeoff between T1 and T1ρ contrast which depends on the resonance offset. We suspect that a similar tradeoff exists for steady-state off-resonance T1ρ contrast, but remains to be explored. In addition, the delivery of off-resonance irradiation generates a magnetization transfer effect and, although magnetization transfer contrast during short TR bSSFP acquisitions has previously been explored (6), it might be possible to saturate off-resonance for applications including CEST imaging. The use of a slSSFP at ultra high field may also have unique applications, for which short TR bSSFP was previously inaccessible because of SAR constraints. Certainly, a low power method for T2-weighted imaging at ultra high field is desirable, since T2-weighted fast spin echo imaging seems significantly handicapped at ultra high field without the use of hyperecho techniques (7).

Conclusion: slSSFP shows promise as a fast imaging technique and was demonstrated here to show T2-weighting at low angle effective fields, which may show some use for ultra high field applications.

References: (1) Li, et al. Magn. Reson. Med. (2005) (2) Witschey, et al. *ISMRM: High Field Systems and Applications.* (2008) (4) Grohn, et al. Magn. Reson. Med. (2003). (5) Ulmer, et al. Am. J. Neuroradiol. (1996).(6) Bieri, et al. Magn. Reson. Med. (2006). (7) Hennig, et al. Magn. Reson. Med (2002).